NUMERICAL STUDY OF THE ERYTHRITOL MELTING PROCESS IN A TRIDIMENSIONAL RECTANGULAR CAVITY

J. F. Raymundo,

R. da S. Borahel,

and R. de C. Oliveski,

Universidade do Vale do Rio dos Sinos

Laboratório de Simulação Numérica

Escola Politécnica

Bairro Cristo Rei

CEP 93.022-000

São Leopoldo, Rio Grande do Sul, Brasil

decesaroo@gmail.com

ABSTRACT

Many areas of engineering, such as the petrochemical and food industries, use thermal energy storage to achieve better performance. Thermal energy storage can be used as a heat source or a heat sink. The thermal storage/release technology, based on the use of phase change materials (PCMs), which possess a great capacity of heat accumulation, has raised an important practical interest. Indeed, the improved storage density and the constant temperature release of energy allow a more compact heat exchange design and simplify system management. Phase change phenomena occurring during PCM melting and PCM solidification need to be carefully controlled. The aim of the present numerical study is to investigate the heat transfer and hydrodynamic characteristics of a phase change material (PCM) in a rectangular cavity and the melting process dependence on the cavity height. The geometry consists of a mini rectangular cavity which contains PCM. Water or steam flows in the longitudinal direction of the cavity, thus heating or cooling the PCM in the cavity. The computational domain is made of three materials: air, aluminum and PCM. The grid mesh is structured, hexaedrical and refined near the walls. The study is developed with different operation conditions of the mass flow and water temperature. The numerical simulation is developed through CFD (Computational Fluid Dynamics) with the Fluent code. The mathematical model was validated using results available in the literature. Results of temperature, velocity and volume fraction fields indicate that the cavity height has no impact on the melting process.

Keywords: PCM, CFD, erythritol

NOMENCLATURE

A	area
A_q	heat transfer area
B	base length
c	mushy zone constant
c_p	specific heat
D	diameter
e	inner fins thickness
H	height
h	enthalpy
h_s	sensible enthalpy
k	thermal conductivity
L	melting enthalpy
mf	melt fraction
p	pressure
S	momentum source term
q	heat transfer rate
q''	heat flux
T	temperature
t	time
V	velocity vector
Vp	pulling velocity
W	width
$\forall$	solid volume

Greek symbols

β	liquid volume fraction
γ	liquid fraction
Δ	difference
γL	enthalpy change due to the phase change
ρ	density
μ	viscosity

Subscripts

s	solid
l	liquid
ref	reference
i	initial
w	wall

INTRODUCTION

Many areas of engineering use thermal energy storage to optimize performance, such as in the cases of petrochemical, food industries and many liquid heating/cooling systems. Thermal energy storage systems can be used as either a heat source or a heat sink. In the applications with intermittent energy generation, such as wasted heat recovery, ground heat

thermal and solar thermal systems, an appropriate thermal storage/release system is essential. The thermal storage/release technology, based on the use of phase change materials (PCMs), which possess a great capacity of accumulating energy for consideration as heat storage media, has raised an important practical interest (Barba and Spiga, 2003). Indeed, the improved storage density and the constant temperature release of energy allow for a more compact heat exchange design and simplified system management. Phase change phenomena occurring during PCM melting and PCM solidification need to be carefully controlled. This effective optimization requires an extensive knowledge of the thermal and dynamic behavior of the fluid within the tanks.

Shatikian et al. (2005) conducted a numerical exploration of the melting process of PCM in an open air rectangular unit with internal fins open to the atmosphere at its top. The melting process occurs at low temperature (23 25 °C) with RT25 paraffin. A parametric investigation is performed in a small system and the temperature of the base varies from 6°C to 24 °C, above the mean melting temperature of the PCM. The results show how the transient process depends on the thermal and geometrical parameters of the system. Dimensional analysis of the results is performed and presented as the Nusselt numbers and melt fractions vs. the Fourier and Stefan numbers. (Rathod et al, 2013).

In terms of PCM, paraffin, for various melting temperatures, has drawn considerable attention of researchers, as well as: Shmueli et al. (2010) and Assis et al. (2007) with RT27, Longeon et al. (2013) with RT35, Al-Abidi et al. (2013) with RT82. In these works, the maximum melting point is 82°C. The properties of paraffin have been investigated up to 90 °C. Thus, for applications where the temperature is above 100 °C, it is not possible to use paraffin.

The aim of the present numerical study is to investigate the heat transfer and hydrodynamic characteristics of a phase change material, (in this case Erythritol), in a rectangular cavity, representing a common TES design. This was done through CFD simulation using the Fluent commercial software.

MATERIALS AND METHODS

The physical problem, the numerical model and the solution method are presented in this section. The validation of the implemented numerical model is presented at the end of this item.

Physical Model

The thermal energy storage (TES) consists of the system presented in Figure 1(a). This system is a square channel with inner fins and filled with PCM inside the cavities. The heat transfer fluid (HTF), water, flows through the external vertical channels

and exchanges heat with the PCM through the aluminum walls.

The system consists of multiple cavities containing Erythritol as PCM, as seen in Figures 1 (a-b).In this case, there is symmetry in the half of the thickness of the inner fins (Figure 2(e)) as well as at the positions that separate the system into four quadrants. In addition, the HTF temperature is kept constant and the metal wall that separates the PCM is thin. With these conditions, we can consider that the temperature of the all vertical walls, between water and PCM, are constant. Thus, it can be considered that the three symmetry regions, shown in Figure 1(b) through the dashed lines. The three-dimensional view of the latter region can be seen in Figure 1(c), which was used as the computational domain of the 3D cases (Figure 1(c)). This calculation domain has dimensions H=200 mm, W=2 mm, B=5 mm and e=0.5 mm. If the TES do not have internal fins, it can be considered that, in the middle cavity, there is no influence on the back and front walls. In this case, the TES can be considered as a 2D problem, as shown in Figure 1 (d).

To take account the volume expansion during solid-liquid phase change due to the large difference in solid and liquid density of PCM, that in reality exists, the cavities were filled with only 180 mm of PCM, the rest was filled with air.

Physical properties of the PCM are needed to conduct the experiment, including its melting point, latent heat capacity (L), density, specific heat and viscosity. Despite extensive research, physical properties were found in only three references (Agyenim et al., 2010, Hesaraki, 2010, and Sillik and Gregson, 2012). In the work of Agyenim et al. (2010) no viscosity values were presented. These values were obtained in the numerical work of Hesaraki (2010). However, the last author used linear variation with temperature for all properties. Sillik and Gregson (2012) presented experimental results of erythritol viscosity, which shows that the variation is logarithmic with the temperature. Therefore, the viscosity values used were the ones presented by Silik and Gregson (2012). The other properties applied were those used by Agyenim et al. (2010) and Hesaraki (2010). Table 1 shows all the properties and values used in this work.

Table 1. Erythritol physical properties.

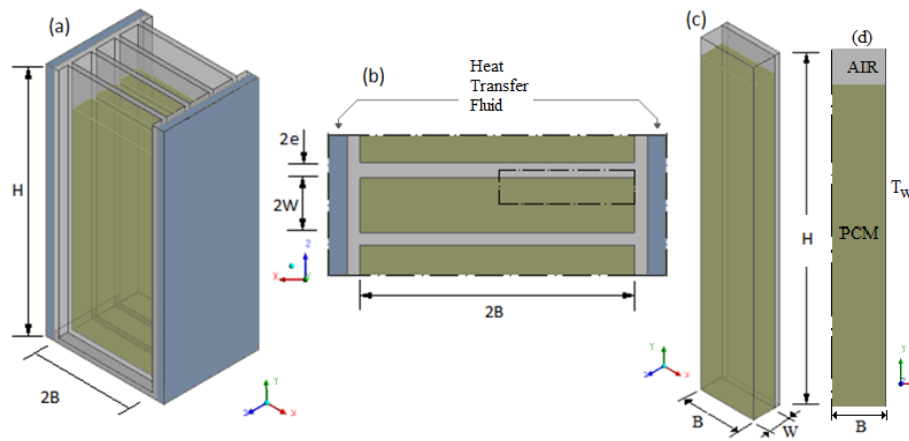| Property	Value
Density (kg m^{-3})	1480 (at 389K); 1300 (at 413 K)
Latent heat capacity (J kg^{-1})	339800
Melting point (K)	391
Specific heat (J kg^{-1} K^{-1})	2250 (at 389 K); 2740 (at 413 K)
Thermal conductivity (W m^{-1} K^{-1})	0.733 (at 389 K); 0.326 (at 413 K)
Viscosity (kg m^{-1} s^{-1})	0.000027749 T²- 0.0231747 T + 4.844

Figure 1. Geometry of the thermal energy storage system: (a) actual geometry; (b) view from top (within dashed line: 3D computational domain); (c) 3D computational domain and (d) 2D computational domain.

Governing equations

The PCM liquid phase is assumed laminar due to the low velocity and small cavity. The conservation equations, utilized in modeling PCM system in Cartesian coordinate system, by enthalpy porosity approach, are (Ye et al., 2011):

$$\frac{D\alpha_n}{Dt} = 0 \qquad (1)$$

$$\rho\frac{D\mathbf{V}}{Dt} = -\nabla p + \mu\nabla\mathbf{V} + \rho\mathbf{g} + \mathbf{S} \qquad (2)$$

$$\rho\frac{Dh}{Dt} = k\nabla^2 T, \qquad (3)$$

where ρ is the density, t is the time, V is the velocity vector, p is the pressure, μ is the dynamic viscosity, S is the momentum source term, h is the enthalpy, k is the thermal conductivity and T is the temperature.

The enthalpy is defined as the sum of the sensible enthalpy (h_s) and the enthalpy change due to the phase change (γL), where h_{ref} is the reference enthalpy at the reference temperature T_{ref}, c_p is the specific heat, L is the specific enthalpy of melting (latent heat of the material), and γ is the liquid fraction during the phase change which occurs over a temperature range $T_s < T < T_l$, where T_s is the solidification temperature and T_l is the melting temperature, defined by the following relation (Shmueli et al., 2010):

$$h_s = h_{ref} + \int_{T_{ref}}^{T} c_p dT \qquad (4)$$

$$\gamma = \begin{cases} 0 & if \ T < T_s, \\ 1 & if \ T > T_l, \\ \dfrac{T - T_s}{T_l - T_s} & if \ T_s < T < T_l, \end{cases} \qquad (5)$$

The enthalpy-porosity technique treats the mushy region (partially solidified region) as a porous medium. The porosity in each cell is set equal to the liquid fraction in that cell. In fully solidified regions, the porosity is equal to zero, which extinguishes the velocities in these regions. The source term in momentum Equation (2) due to the reduced porosity in the mushy zone takes the following form (ANSYS-FLUENT):

$$S = \frac{c(1-\beta)^2}{(\beta + \varepsilon)}(\mathbf{V} - \mathbf{V}_p) \qquad (6)$$

where β is the liquid volume fraction, ε is a small constant ($= 0.001$) to avoid division by zero, c is the mushy zone constant and V_p is the solid velocity due to the pulling of solid phase out of the domain. Studied by some researchers (Voller and Prakash, 1987, Brent et al. 1988, Shmueli et al., 2010, among others), c is a constant that depends of the morphology of the mushy zone (Voller and Prakash, 1987).

The numerical simulations of the melting were carried out using the commercial software ANSYS FLUENT-14. The Equations (1-6) were solved for each point at the computational domains. PRESTO scheme was used for the pressure correction equation, PISO for pressure–velocity coupling and Second

Order Upwind to solve the momentum and energy equations.

The melt fraction (mf) and the heat transfer rate (q) (Equations following, respectively) are obtained as shown in (Shmueli et al., 2010):

$$q = -\rho \frac{d\forall(t)}{dt} \qquad (7)$$

$$mf(t) = 1 - \frac{\forall(t)}{\forall(t=0)} \qquad (8)$$

where $\forall$ is the solid volume. The heat flux (q"=q/A) was obtained considering the areas of solid walls that exchange heat with the PCM. In this case, for the 2D and 3D computational domains, respectively, these areas were: $A_{q2D}=H_{PCM}W$ and $A_{q3D}=H_{PCM}(W+B)$.

NUMERICAL PROCEDURES

The numerical domain boundary conditions, post processing methods and numerical validations are presented in this section.

Boundary Conditions

The initial temperature of the air inside the cavity is equal to the initial temperature of the PCM (389 K). The numerical simulations were carried out for three temperature differences (ΔT) between Tw and initial temperature (Ti) of the PCM: 10, 15 and 20 °C. All rigid walls were assumed as no slipping. The bottom wall was assumed as adiabatic. A constant and uniform temperature was prescribed at the heating wall (Tw). The symmetry condition was used on all other walls. In the 3D case it was used as the couple-wall boundary condition at the interface between PCM and fin to allow the conjugate heat transfer.

The computational domain consists of a cavity partially filled with PCM, while the rest is filled with air. This was done to allow the PCM volume expansion during heating. Thus, with the expansion of the PCM, a certain quantity of air must leave the cavity. At the cavity's top, the Pressure-Outlet condition was used, with Gauge Pressure = 0 and Backflow Temperature = Tw. All spatial meshes were hexaedrical and constructed with the multi-block methodology and refinement near the solid walls and the PCM-air interface.

Post Processing Method

Post processing was done through the ANSYS CFX-Post software. The remaining solid PCM volume for each time was obtained through mass fraction iso-surfaces, where the volume below the iso-surface is the solid PCM value. The melt fraction is then obtained using Equation 8.

Numerical Model Validation

The numerical validation was done using the results of Shmueli et al. (2010). The study consists of PCM melting in a vertical cylindrical tube. Two tube diameters (D) equal to 3 and 4 cm were used, with total height (H) of 20 cm. Only 17 cm were filled with PCM, to allow its expansion, while the remaining 3 cm were filled with air. The walls temperatures were either 10 or 30 °C above the PCM's melting temperature. The PCM used by Shmueli et al. (2010) was RT27.

Quantitative validation is shown in Figure 2, which shows results of the melt fraction vs. time obtained by Shmueli et al. (2010) and this study. A very small difference can be observed in the early and final stages, however, almost no difference is present during the remaining time of the melting process. With this result, we can consider the numerical model as validated.
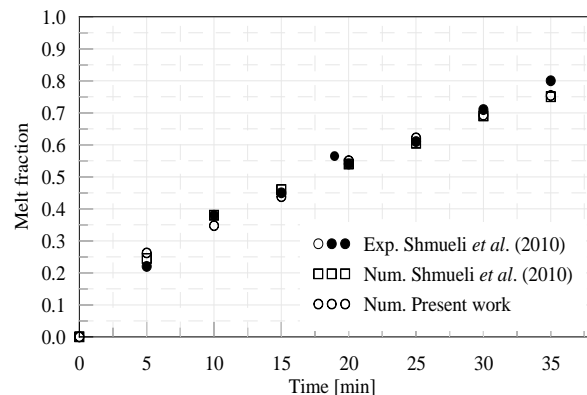

Figure 2. Melt Fraction vs Time, Experimental and numerical results of Shmueli et al. (2010) and the present work.

RESULTS AND DISCUSSION

The two computational domains (2D and 3D) were tested with 3 spatial grids and three time steps (0.05, 0.01, 0.005 s). No significant difference was observed between the results obtained with time steps of 0.005 and 0.01 s. Also three spatial grids were tested for each model. For the 2D problem (Figure 1 (e)), the grids have approximately: $2.6\text{x}10^3$, $4.8\text{ x}10^3$ and $6.2\text{ x}10^3$ elements; and for the problem 3D (Figure 1 (d)): 4x104, 9.1 x104 and 22.6 x104 elements. In both cases, no significant differences were found between the finer and medium grids. Thus, the results presented here were obtained with the medium value of spatial grid ($4.8\text{ x}10^3$ and 9.1 x104) and time step (0.01 s).

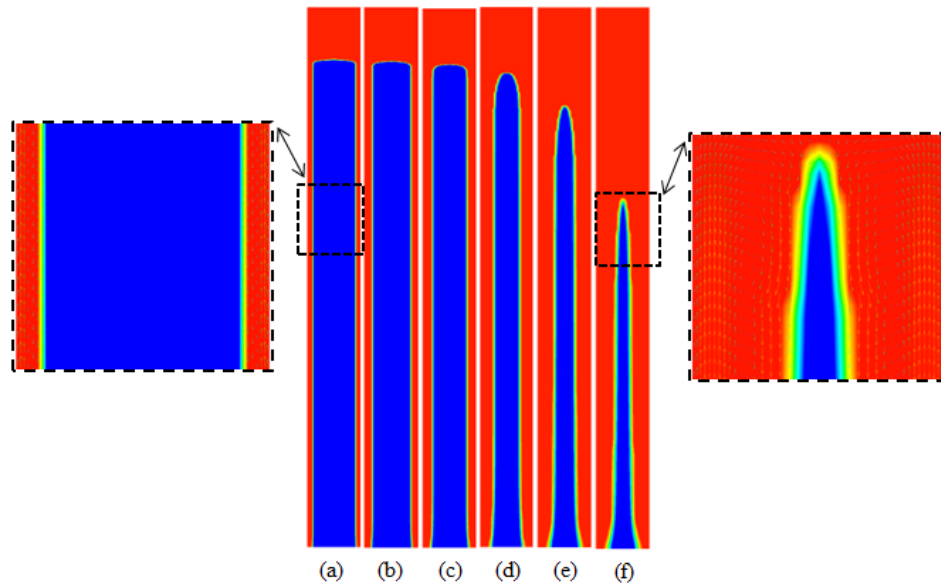Figure 3. Melt fraction vs. time. 2D and ΔT=10 ºC: (a) 1 min, (b) 2 min; (c) 3 min; (d) 6 min; (e) 9 min; (f) 12.

Figures 3 (a-f) show the fraction melting field for various time steps (1- 12 min). Red and blue colors represent the portions of liquid and solid, respectively. In these figures, it can be seen that, in the first moments, there is almost no variation of the solid height. This occurs because, in the early stages, the heat transfer process occurs mainly by conduction. Later, the natural convection process is increased, thus causing greater PCM melting. We can observe these conditions comparing the velocity representation of the Figures 3 (a, f) details, where we can observe that the upstream and downstream flow of the latter (Figure 3(f)) are much greater than the first (Figure 3(a)). Finally, one can clearly identify the shear layer between the two flows and the complete representation of velocity profiles, which demonstrates the good quality of the grid used.

Figures 4 (a-b) shows, respectively, the melting fractions as a function of time for the 2D and 3D models, for ΔT equals to 10, 15 and 20 °C. In both cases, it can be observed that the higher the ΔT, the faster is the PCM reaches a certain melt fraction. For the 3D case, for the example, with ΔT equal to 10 °C, 0.5 melt fraction is achieved in 24 seconds, while with ΔT equal to 20 °C, the same melt fraction is achieved in 12 seconds.

When comparing both cases (2D (a) and 3D (b)), a severe difference in total melting time is noticed. This difference is due to the presence of an internal fin in the 3D case, greatly increasing of the total heat transfer area. In this case, the melting fraction equal to 0.9 is reached after 70, 85 and 108 seconds for ΔT=20, 15 and 10 °C, respectively. This indicates that the time for a certain melt fraction to be reached in the 3D domain for the same ΔT is approximately 7 times that of the 2D domain, considering the depth of the TES (W) as 2 mm.
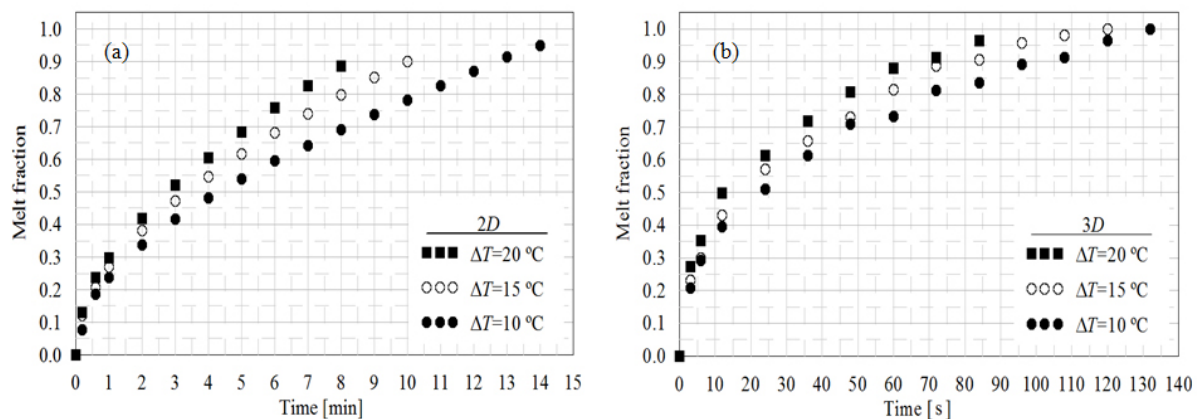

Figure 4. Melt fraction vs. time for cases with ΔT=10, 15 and 20 °C, 2D (a) and 3D with W=2 mm (b).

The comparison between different values of H for the tridimensional case is presented in Figure 5. Three values of H for the same case with W=2 mm and ΔT=20 °C are presented. This represents how the PCM behaves as the total height of the TES increases. It is noticed that the height has little influence on the time required for the PCM to reach a certain melt fraction, as well as the total melting time. This occurs because as the height is increased, the total heat exchange area is increased and this process is effective enough so that the volume increase does not increase the total melting time.

Figure 6 shows the mean heat flux (q'') as a function of time for the same cases as Figure 5. As expected, the heat flux transferred to the PCM decreases with time and is maximum at the beginning and minimum when the solidification is complete. It
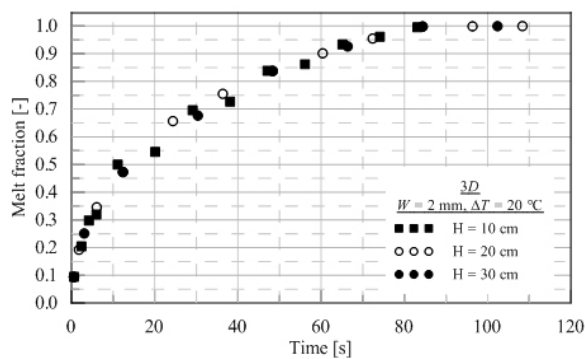
is not possible to observe a significant difference between the cases with different heights.

Figure 7 shows the results of melt fraction as a function of time for a case where the spacing between the fins (W) is 4 mm, ΔT= 15 °C and H=10, 20 and 30 cm. Even when changing other operation conditions, it is not possible to observe significant changes in the melting curves in the cases with different height values. This shows that the cavity's height does not affect the melting time despite some other variables, such as the spacing between the fins (W) and the temperature difference (ΔT). It is important to notice that the height does, in fact, increase the total energy stored in the system, in a way that it should be considered in future projects, however it does not change the melting times.

Figure 5. Melt fraction vs. time. 3D, ΔT=20 °C, W=2 mm and H=10, 20 and 30 cm.
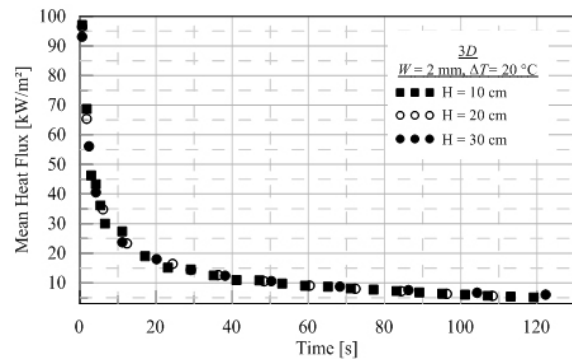

Figure 6. Mean Heat Flux vs. time. 3D, ΔT=20 °C, W=2 mm and H=10, 20 and 30 cm.

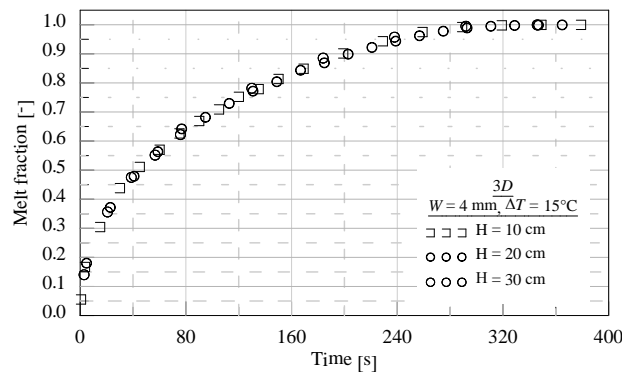

Figure 7. Melt fraction vs. time. 3D, ΔT=15 °C, W=4 mm and H=10, 20 and 30 cm.

CONCLUSIONS

The aim of this numerical study was to investigate the heat transfer and hydrodynamic characteristics of a phase change material (PCM) in a vertical rectangular cavity with inner fins. The study was developed assuming different wall temperatures and different spacing between the fins, using Erythritol as PCM. The numerical simulation was conducted through Computational Fluid Dynamics (CFD) with the Fluent code. The mathematical model

was validated using the results of Shmueli et al. (2010), in terms of melt fraction as a function of time. The results displayed proper qualitative and quantitative agreement. Therefore it can be concluded that the numerical model implemented here is appropriate. The 3D domain of a rectangular cavity were simulated for three different ΔT values (10, 15 and 20 °C) and three values of W (2, 3 and 4 mm). The results obtained through melt fraction as a function of time showed that the higher the ΔT, the lowest the time required for higher melt fractions to

be achieved. It's noticed that the cavity's height doesn't influence the total melting time in a significant way, regardless of the distance between the inner fins and the temperature difference between the system's walls and the melting temperature of the PCM. It can be concluded that the height of the system does not interfere in the speed in which is PCM melts, but it does directly influence the system's energy storage capacity, due to the increase in PCM volume contained.

ACKNOWLEDGEMENTS

REFERENCES

Agyenim, F., Eames, P., and Smyth, M., 2010, Heat Transfer Enhancement in Medium Temperature Thermal Energy Storage System using a Multitube Heat Transfer Array, Renewable Energy, Vol. 35, pp. 198-207.

Al-Abidi, A. A., Mat, S., Sopian, K., Sulaiman, M. Y., and Mohammad, A. T., 2013, Internal and External Fin Heat Transfer Enhancement Technique for Latent Heat Thermal Energy Storage in Triplex Tube Heat Exchangers, Applied Thermal Engineering, Vol. 53., pp. 147-156.

Ansys, 2011, *Fluent, Release 14.0*, Solver Modeling Guide.

Assis, E., Katsman, L., Ziskind, G., and Letan, R., 2007, Numerical and Experimental Study of Melting in a Spherical Shell, International Journal of Heat and Mass Transfer, Vol. 50, pp. 1790-1804.

Barba, A., and Spiga, M., 2003, Discharge mode for Encapsulated PCMs in Storage Tank, Solar Energy, Vol. 74, No. 2., pp. 141-148.

Brent, A. D., Voller, V. R., and Reid, K. J., 1988, Enthalpy-Porosity Technique for Modeling Convection-Diffusion Phase Change: Application to the Melting of a Pure Metal, Numerical Heat Transfer, Vol. 13, pp. 297-318.

Hesaraki, A., 2011, *CFD Modeling of Heat Charging Process in a Direct-Contact Container for Mobilized Thermal Energy Storage*, Lambert.

Longeon, M., Soupart, A., Fourmigué, J. F., Bruch, A., and Marty, P., 2013, Experimental and Numerical Study of Annular PCM Storage in the Presence of Natural Convection, Applied Energy, Vol. 112, pp. 175-184.

Rathod, M. K., and Benerjee, J. R., 2013, Thermal Stability of Phase Change Materials used in Latent Heat Energy Storage Systems: a Review, Renewable and Sustainable Energy Reviews, Vol. 18, pp. 246-258.

Shatikian, V., Ziskind, G., and Letan, R., 2005, Numerical Investigation of a PCM-based Heat Sink with Internal Fins, International Journal of Heat and Mass Transfer, Vol. 51, pp. 1488-1493.

Shmueli, H., Ziskind, G., and Letan, R., 2010, Melting in a Vertical Cylindrical Tube: Numerical Investigation and Comparison with Experiments, International Journal of Heat and Mass Transfer, Vol. 53, pp. 4082-4091.

Sillick, M., and Gregson, C. M., 2012, Spray Chill Encapsulation of Flavors within Anhydrous Erythritol Crystals, LWT-Food Science and Technology, Vol. 48, No. 1, pp. 107-113.

Voller, V. R., and Prakash, C., 1987, A Fixed Grid Numerical Modeling Methodology for Convection-Diffusion Mushy Region Phase-change Problems, International Journal of Heat and Mass Transfer, Vol. 30, pp. 1709-1719.

Ye, W. B., Zhu, D. S., and Wang, N., 2012, Fluid Flow and Heat Transfer in a Latent Thermal Energy Unit with Different Phase Change Material (PCM) Cavity Volume Fractions, Applied Thermal Engineering, Vol. 42, pp. 49-57.